

# PilotANN: Memory-Bounded GPU Acceleration for Vector Search

Yuntao Gui<sup>1</sup> Peiqi Yin<sup>1</sup> Xiao Yan<sup>2</sup> Chaorui Zhang<sup>3</sup> Weixi Zhang<sup>3</sup> James Cheng<sup>1</sup>

## Abstract

Approximate Nearest Neighbor Search (ANNS) has become fundamental to modern deep learning applications, having gained particular prominence through its integration into recent generative models that work with increasingly complex datasets and higher vector dimensions. Existing CPU-only solutions, even the most efficient graph-based ones, struggle to meet these growing computational demands, while GPU-only solutions face memory constraints. As a solution, we propose PilotANN, a hybrid CPU-GPU system for graph-based ANNS that utilizes both CPU’s abundant RAM and GPU’s parallel processing capabilities. Our approach decomposes the graph traversal process of top- $k$  search into three stages: GPU-accelerated subgraph traversal using SVD-reduced vectors, CPU refinement and precise search using complete vectors. Furthermore, we introduce fast entry selection to improve search starting points while maximizing GPU utilization. Experimental results demonstrate that PilotANN achieves 3.9–5.4 $\times$  speedup in throughput on 100-million scale datasets, and is able to handle datasets up to 12 $\times$  larger than the GPU memory. We offer a complete open-source implementation of PilotANN: <https://github.com/ytgui/PilotANN>.

## 1. Introduction

Approximate Nearest Neighbor Search (ANNS) is a fundamental vector search technique that efficiently identifies similar items in high-dimensional vector spaces. Given a query vector, ANNS returns its  $k$ -nearest neighbors by making controlled accuracy and search speed trade-offs. This balance between accuracy and speed has made ANNS the de facto solution for large-scale similarity search prob-

<sup>1</sup>The Chinese University of Hong Kong, Hong Kong SAR  
<sup>2</sup>Centre for Perceptual and Interactive Intelligence, Hong Kong SAR  
<sup>3</sup>Theory Lab, 2012 Labs of Huawei Technologies Co. Ltd.  
 Correspondence to: Yuntao Gui <ytgui@cse.cuhk.edu.hk>.

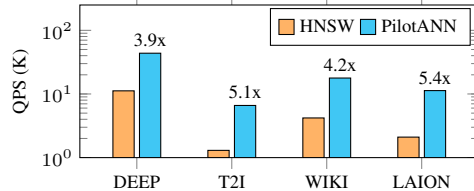


Figure 1. Recall@10=0.90 QPS on 100 million datasets.

lems where exact nearest neighbor computation would be computationally prohibitive. Traditionally, ANNS has served as the backbone for retrieval engines (Kulis & Grauman, 2009; Gordo et al., 2016) and recommendation systems (Covington et al., 2016; He et al., 2017; Yang et al., 2020). More recently, ANNS has gained renewed prominence through its integration into generative AI systems, where it enhances both truthfulness and efficiency, e.g., retrieval augmented generation (Lewis et al., 2020; Blattmann et al., 2022), and semantic cache (Bang, 2023).

The computational requirements of ANNS continue to grow with recent advances in generative AI, particularly as modern Transformer-based architectures work with higher-dimensional embeddings and larger-scale datasets (Devlin et al., 2018; Dosovitskiy et al., 2021; Radford et al., 2021). While deep learning systems can be easily replicated and scaled horizontally due to their stateless nature, ANNS typically remains centralized, making single-machine throughput a critical bottleneck. Using 100-million scale datasets with dimensions ranging from 96 to 768, we observe that state-of-the-art CPU implementation of HNSW (Malkov & Yashunin, 2020) struggles to maintain high query throughput as vector dimensions increase (Figure 1). Specifically, for the LAION dataset with 768-dimensional vectors, CPU-only HNSW can only process 2.1K queries per second (QPS). This low throughput becomes particularly problematic for production services that need to handle thousands of concurrent requests, where maintaining high processing throughput is essential.

Previous attempts to enhance graph-based ANNS efficiency have explored several approaches. One direction focuses on developing fine-grained graph construction methods (Fu et al., 2019; Lu et al., 2021). While these methods improve search efficiency, they often require inten-

sive computational resources during the build phase and face scalability challenges with large-scale datasets (Chen et al., 2021). Another approach employs quantization techniques (Jégou et al., 2011a; Zhou et al., 2012; Douze et al., 2018) to compress vector representations, reducing memory footprint and computational costs. However, quantization inevitably introduces accuracy degradation, presenting a fundamental trade-off on search accuracy.

GPU acceleration represents a promising direction for enhancing ANNS performance (Zhao et al., 2020; Zhu, 2022; Ootomo et al., 2023). However, leveraging GPUs is a non-trivial endeavor despite their massive parallel processing capabilities. The primary limitation is GPU memory capacity, which constrains the size of datasets that can be processed. NVIDIA’s state-of-the-art GPU-based ANNS library CAGRA (Ootomo et al., 2023), requires expensive GPU hardware with large memory capacity (e.g., A100) to handle moderate-sized datasets. While unified virtual memory (UVM) has been explored as a solution for memory constraints, previous work has shown its ineffectiveness in non-graph ANNS (Zhang et al., 2024). Graph-based ANNS presents additional challenges due to its dynamic nature and irregular memory access patterns (see §2.2), making efficient GPU utilization particularly difficult.

These limitations have created a clear need for a hybrid approach that can utilize both CPU and GPU capabilities effectively. In response, we present PilotANN, a hybrid system for graph-based ANNS designed to harness both the parallel processing power of the GPU and the abundant RAM available on the CPU. Our approach specifically addresses two fundamental challenges:

- **C1: GPU memory boundaries.** The limited memory capacity of a GPU, typically in the tens of gigabytes, is significantly smaller than that of the CPU, which can exceed hundreds of gigabytes, thus restricting the applicability of ANNS on the GPU.
- **C2: Limited computational density.** GPUs are optimized for complex matrix-matrix operations (e.g., GEMM), but ANNS primarily relies on simpler pairwise distance calculations, resulting in low computational density on the GPU.

PilotANN tackles these challenges through two key innovations. First, we introduce **Multi-stage ANNS Processing** (§4), which decomposes the computationally intensive top- $k$  search problem into complementary components: leveraging GPU power to efficiently identify candidates on smaller sub-graphs, followed by refinement and precise traversal on the CPU, where the complexity of ANNS is significantly reduced. Second, we develop **Fast Entry Selection** (§5), a novel method that provides high-quality entry points for search, resulting in increased com-

putational density on the GPU. Our experimental evaluation, conducted using only one NVIDIA A10 GPU (24 GB), demonstrates significant performance improvements. We achieve a throughput speedup of  $3.9 - 5.4\times$  for top-10 searches, while handling datasets and graph index up to  $12\times$  larger than the GPU’s memory capacity.

The contributions of this work are threefolds:

- We introduce a novel hybrid architecture that effectively enables GPU acceleration for CPU-based ANNS.
- We develop fast entry selection, a GPU-efficient method for optimizing entry point selection.
- We provide comprehensive empirical evidence of PilotANN’s effectiveness on real-world datasets.

## 2. Background

In this part, we introduce the basics of ANNS and graph traversal algorithm to facilitate the subsequent discussions.

### 2.1. ANNS Methods

The goal of ANNS is to efficiently find the data points in a given dataset  $X$  that are closest to a query point  $q$  according to a distance metric (Chen et al., 2021; Peng et al., 2023; Douze et al., 2024). Modern ANNS methods can be broadly categorized into two main approaches: non-graph methods based on coarse clustering, and graph-based methods that rely on fine-grained graph connectivity.

*Traditional non-graph methods* employ coarse clustering as their foundational principle, partitioning the search space to reduce computational complexity during query time. This includes techniques like space-partitioning KD-tree (Silpa-Anan & Hartley, 2008) that recursively divide the space into hierarchical regions, and locality-sensitive hashing (Gionis et al., 1999) that groups similar vectors into buckets. The most direct application of clustering is the Inverted File (IVF) method (Jégou et al., 2011b), which explicitly partitions vectors using k-means into inverted lists. Advanced variants like IMI (Babenko & Lempitsky, 2015) employ product clustering to create finer partitions, while IVFADC (Schütze et al., 2008; Jégou et al., 2011a) combines clustering with residual quantization. However, these coarse clustering methods face an inherent trade-off between search complexity and partition granularity.

*Graph-based methods* take a fundamentally different approach by constructing a navigable graph structure (Hajebi et al., 2011; Malkov et al., 2014), where each data point is represented as a node and edges connect neighboring nodes. During search, these methods perform graph traversal to quickly locate nearest neighbors. Modern approaches like HNSW (Malkov & Yashunin, 2020) organize the proximity graph into multiple layers for coarse-to-fine search,

**Algorithm 1** ANNS by Greedy Search

---

```

1: Input: graph  $G(V, E)$ , query  $q$ , entry points  $EP$ , candidate size  $ef$ 
2: Output:  $C$  contains  $ef$  nearest neighbors
3: priority queue  $C \leftarrow EP$ 
4: repeat
5:    $u \leftarrow$  the first unchecked node in  $C$ 
6:   for unvisited  $v \in \{v | (u, v) \in E\}$  do
7:     mark  $v$  as visited
8:      $d \leftarrow \text{euclidean}(q, v)$ 
9:      $C.\text{insert}(v)$  w.r.t.  $d$ 
10:  end for
11:   $C.\text{resize}(ef)$ 
12: until  $C$  has no unchecked node
    
```

---

while NSG (Fu et al., 2019) optimizes graph connectivity for better search routes. Studies have consistently shown that graph-based methods achieve state-of-the-art performance in terms of the accuracy-throughput trade-off, requiring fewer distance computations than traditional coarse clustering methods to achieve the same recall rates (Douze et al., 2018; Chen et al., 2021). This superior performance stems from their ability to capture fine-grained neighborhood connections and perform guided graph traversal, which makes graph-based approaches highly optimized. Exploring further improvements on graph-based methods remains an active area of research (Zhao et al., 2020; Ootomo et al., 2023; Karthik et al., 2024).

## 2.2. Revisiting Graph Traversal

Graph-based ANNS typically employs a heuristic greedy search algorithm 1. This algorithm explores the graph efficiently by maintaining a restricted number of the most promising candidate solutions at each step, thereby limiting computational complexity.

The algorithm begins by constructing a candidate list  $C$  (line 3) containing the most promising solutions identified during the search process. This list comprises  $ef$  candidates, from which the top- $k$  results ( $k \leq ef$ ) can be obtained later. Here the  $ef$  serves as a parameter to control search accuracy and speed. In each subsequent iteration, the search begins by expanding the best unchecked candidate in  $C$  (line 5-6), computing distances of unvisited neighboring nodes to the query vector  $q$  (line 8), and updating  $C$  as potential solutions (line 9). This iterative process continues until all nodes in  $C$  have been checked (line 4), indicating that no further improvement is possible within the current search space.

The greedy search algorithm exhibits two key characteristics. First, at each neighbor expansion iteration, the algorithm selects the best candidate from the dynamically

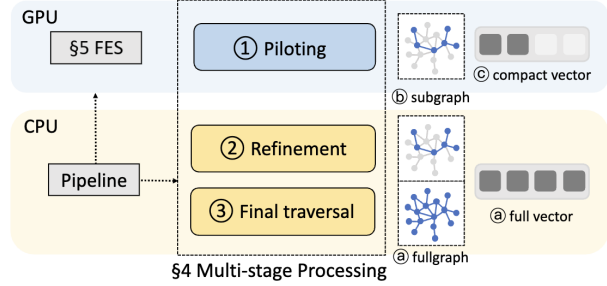


Figure 2. Architecture of PilotANN.

changing  $C$ , making the traversal path unpredictable. This dynamic nature with **C1** motivates most of the system design. Second, The algorithm primarily performs vector-to-vector distance calculations (line 8), which are simple element-wise operations that cannot utilize the GPU’s matrix multiplication (GEMM) capabilities, i.e., **C2**.

## 3. Overview

PilotANN employs a unique hybrid CPU-GPU processing paradigm that leverages the distinct advantages of both hardware. Figure 2 illustrates the system’s architecture and core components.

The key insight of PilotANN is to decompose the ANNS process into complementary stages that run on both GPU and CPU. During preprocessing, given the full index ④, we sample a smaller subgraph ⑥ and generate compact vector representations ③. The smaller subgraph and compact vectors can fit within GPU memory, while the original full index kept in CPU RAM. At runtime, PilotANN processes queries through our multi-stage processing method (§4), where the GPU stage ① enables efficient initial exploration, and the CPU stages ②③ benefit from reduced search complexity. Moreover, fast entry selection (FES §5) is designed to improve the quality and speed of initial starting point selection. Together, PilotANN is able to achieve high throughput while effectively processing datasets that significantly exceed GPU memory capacity.

## 4. GPU Piloting: A Hybrid Approach

### 4.1. Multi-stage Processing of ANNS

PilotANN introduces a novel approach to vector search through a “**staged data ready processing**” paradigm. Unlike traditional GPU-enabled systems that adhere to a “move data for computation” model, our method minimizes data movement by ensuring data readiness across processing stages. This design choice is particularly crucial due to the inherent characteristics of graph traversal algorithm shown in §2.2. During iterative neighbor expansions,

the search path becomes data-dependent and unpredictable, which would necessitate intensive data transfers over PCIe in conventional architectures.

Our method breaks down the search into three distinct stages: (i) GPU piloting with subgraph and reduced vectors, (ii) residual refinement with subgraph and full vectors, and (iii) final traversal with full graph and vectors. Beginning with a query and entry points, the system sequentially executes these stages to locate top- $k$  matching results.

**① GPU piloting.** In the first stage, we employ dimensionality reduction and graph sampling to enable GPU-based traversal under memory constraints. For dimensionality reduction, we apply singular value decomposition (SVD) to the original vectors:  $X = U\Sigma V^T$ , where  $V^T V = I$  ensures the orthogonality of the transformation, preserving Euclidean distances. Each vector is decomposed into two components:  $\hat{x} = \{x_{primary}, x_{residual}\}$ , where  $x_{primary} = \{U_{1,\dots,d}\Sigma_{1,\dots,d}\}$ , captures the principal components with  $d$  highest singular values, and  $x_{residual}$  contains the remaining components. The graph sampling process employs uniform node-wise sampling to select seed nodes, followed by 1-hop neighbor expansion to include frontier nodes, until reaching a target sampling ratio; the sampled nodes are then reconnected using the same graph construction algorithm as the original index.

**② Residual refinement.** This intermediate stage enhances the GPU results by incorporating the previously omitted residual vector components. For each candidate identified in ①, we calculate complete distance by combining the GPU-computed  $x_{primary}$  distance with the  $x_{residual}$  distance. The stage then performs a limited graph traversal (2 iterations) on the subgraph, re-ranking candidates based on their full-dimensional distances and generating a visited table. This refinement process produces two key outputs: a more accurately ranked candidates and a visitation history that guides the subsequent complete graph exploration.

**③ Final traversal.** The final stage performs a complete graph search using full-dimensional vectors, ensuring search quality and completeness. Building upon the previous stages’ outputs, it proceeds a traditional greedy search algorithm §2.2 with two key advantages: a pre-populated visited table and high-quality initial candidates. By reusing the visited table, the search avoids revisiting previously explored nodes. The quality of starting points obtained from earlier stages significantly improves traversal efficiency, see §4.2.

**Summary.** Our design is cost-effective as it requires only a single GPU, while scaling well across vector dimensions and graph complexity. Data transfer overhead is minimal – only the query vector moves to GPU memory initially, and a small candidate set (typically less than 1KB per query)

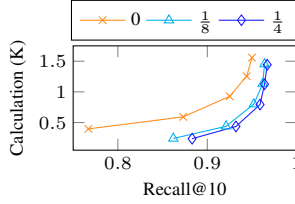


Figure 3. Calculation requirements of LAION-1M under different  $\frac{\tau}{ef}$  conditions.

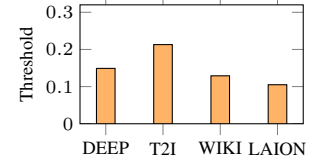


Figure 4. Acceleration thresholds to obtain  $2\times$  distance calculation savings.

returns to CPU after ①. The design ensures search quality through graceful degradation: if only the final stage operates, the system functions as a traditional greedy search, while bringing speedups when all stages work together.

## 4.2. Understanding the Performance

Our approach demonstrates effectiveness through two aspects. First, the GPU stage ① can significantly reduce search complexity for subsequent CPU stages ②③. Second, the GPU’s massive parallel processing capabilities are essential for our approach, as they enable efficient graph traversal that ensures multi-stage overheads do not compromise its benefits. We validate these claims through the following performance analysis.

**Reduced search complexity.** Our method builds upon a simple but powerful observation: graph-based top- $k$  search becomes much more efficient when it begins with some ground truth results already known. To measure this effect, we conducted experiments with HNSW using 32 neighbors per node, comparing searches initialized with or without partial ground truth. Specifically, for the former, we construct initial search candidate of size  $ef$  by combining  $\tau$  known correct results with  $ef - \tau$  randomly selected nodes.

Figure 3 demonstrates the substantial benefits of this approach. When starting with  $\frac{\tau}{ef} = \frac{1}{4}, \frac{1}{8}$ , the search only requires 39.9% and 48.1% distance calculations to reach a recall of 0.90 compared to search without ground truth. This improvement happens because the search immediately focuses on promising areas of the graph, avoiding wasted effort in exploring less relevant regions. We observe similar improvements across different datasets, showing its generalizability. In the proposed design, the first two stages ①② utilizing GPU’s parallel processing power to rapidly identify high-quality neighbors that serve as approximate ground truth, accelerating the final stage ③.

This benefit only materialize when identifying a sufficient proportion of ground truth neighbors. We define *acceleration threshold* as the minimum ratio  $\frac{\tau}{ef}$  needed to achieve meaningful speedup (e.g.,  $2\times$ ). As Figure 4 reveals, this threshold varies across datasets, typically requiring 15-21%

Table 1. Stage breakdown on LAION-1M.

Method	Stage ①	Stage ②	Stage ③
HNSW	-	-	668.8
Multi-stage	574.2	44.2	189.0

of ground truth results. This minimum threshold requirement guides our system design – we employ both graph sampling and vector dimensionality reduction to maximize the subgraph size that can fit within limited GPU memory.

**Stage breakdown.** A breakdown of distance calculations across stages reveals why GPU acceleration is fundamental to our design (Table 1). While the baseline HNSW requires 668.8 calculations to reach a recall of 0.9, our method distributes its workload across three stages: 574.2 calculations in the initial GPU stage, followed by 44.2 and 189.0 calculations in two CPU stages. The CPU-executed portions, totaling 233.2 calculations on ②③, are  $3.3\times$  smaller than the baseline, which is the key to our acceleration. Although the Multi-stage involves more calculations in total, the GPU’s parallel processing capabilities handle the increased workloads of ① efficiently. Specifically, we measure vector-to-vector distance computation on CPU and GPU, the GPU is capable of handling  $82\times$  more computations over a single CPU core. We further optimize system throughput by processing queries in batches and pipelining their execution across CPU and GPU stages.

### 4.3. Methodology Details

**Subgraph management.** The subgraph representation employs a modified Compressed Sparse Row (CSR) format that optimizes memory usage while maintaining efficient mapping between the subgraph and full graph. Rather than completely removing nodes excluded during sampling, we retain their presence in the CSR structure but remove their connectivity information and embedding vectors. These nodes are represented with zero out-degree, and any incoming edges are pruned. This design makes the data structure on the GPU have a little redundancy (these zero-degree nodes), however, it avoids the computational overhead of node ID mapping between subgraph and fullgraph representations, resulting in improved CPU performance.

**Visited table management.** Our GPU kernel utilizes bloom filters to track visited nodes, with the filter states stored in shared memory. This design eliminates the need for dynamic memory allocation and reduces DRAM access overhead. While bloom filters are known to produce false positives – incorrectly marking unvisited nodes as visited – this limitation does not compromise our system’s correctness. Our multi-stage processing pipeline ensures accuracy by refining GPU results on the CPU side, where any false

Table 2. Complexity of distance computations.

Method	Comp.	Mem. read	Density
Brute force	$mnd$	$md + nd$	$\frac{mn}{m+n}$
Graph traversal	$mnd$	$md + mnd$	$\frac{n}{1+n}$
FES (general)	$\frac{mnd}{r}$	$md + nd$	$\frac{mn}{r(m+n)}$
FES (1 block)	$mnd$	$md + nd$	$\frac{mn}{m+n}$
FES (1 query)	$\frac{nd}{r}$	$d + \frac{nd}{r}$	$\frac{n}{1+n}$

positive nodes are properly revisited.

## 5. Fast Entry Selection

In graph-based ANNS, the search begins with entry points before executing graph traversal. These entry points can be predefined nodes (Malkov & Yashunin, 2020) or randomly selected points (Fu et al., 2019). We introduce Fast Entry Selection (FES), a novel method optimized for GPU execution that operates before §4. FES employs GEMM-like high-density distance computations to improve entry point quality without compromising search speed, thereby enhancing overall system efficiency.

**Computational density.** We first examine computational density w.r.t. the roofline performance model (Williams et al., 2009). Given vector dimension  $d$ , we have  $m$  query vectors  $Q \in \mathbb{R}^{m \times d}$  and  $n$  entry vectors  $EV \in \mathbb{R}^{n \times d}$ . As listed in Table 2, a straightforward brute force approach computes the distance between each query and entry vector, resulting in an  $m \times n$  matrix  $D$ , where each element represents the distance between one query vector and one entry vector. Treating the squared euclidean distance computation  $euclidean(x_1, x_2) = (x_1 - x_2)^2$  as a single computation, the entry stage involves  $mnd$  computations with  $md + nd$  memory reads, the ratio between computation and memory access is  $\frac{mn}{m+n}$ , i.e., computational density.

During neighbor expansion (lines 6-10 in Algorithm 1), computing the same distances  $D$  requires  $md + mnd$  memory reads for query vectors  $Q$  and neighbor vectors  $V \in \mathbb{R}^{m \times n \times d}$ , where each of the  $m$  queries has different  $n$  neighbors. This yields a computational density of  $\frac{n}{1+n}$ , significantly lower than  $\frac{mn}{m+n}$  as  $m$  increases. A comparable scenario during the graph construction process, namely local-join, was also reported (Dong et al., 2011). This observation motivates us to explore novel methods that can maintain high computational density while reducing the effective search space.

**Clustering-based selection.** Inspired by IVF, we propose a simplified and bucket-aligned approach optimized for entry point selection. Our method organizes entry vectors into a small number of coarse clusters ( $r$ ), enabling efficient GEMM-like computations on GPUs. Unlike IVF, which

**Algorithm 2** Tiled FES GPU Kernel

---

```

1: Input: queries  $Q[m][d]$ , entry vectors  $EV[r][n/r][d]$ 
2: Output: distances  $D[m][n]$ 
3: parallel for  $block \leftarrow$  loop  $r$  GPU blocks
4: for  $j \leftarrow$  loop  $n/r$  entry vectors, stride=32 do
5:   for  $k \leftarrow$  loop vector dimension  $d$ , stride=32 do
6:      $rhs \leftarrow EV[block][j : j + 32][k : k + 32]$ 
7:     parallel for  $i \leftarrow$  loop  $m$  queries
8:     if  $Q[i]$  not closest to  $block$  then
9:        $continue$  {Skip non-active query}
10:    end if
11:     $lhs[i\%32] \leftarrow Q[i][k : k + 32]$ 
12:     $synchronize()$  {Memory barrier}
13:     $D_{partial} \leftarrow euclidean(lhs, rhs)$ 
14:     $D[i][j] \leftarrow D[i][j] + D_{partial}$ 
15:    end parallel for
16:     $synchronize()$  {Wait all queries to finish}
17:  end for
18: end for
19: end parallel for

```

---

typically employs thousands of buckets with highly variable sizes, our method deliberately uses a small number of coarse clusters ( $r \ll$  IVF buckets). For queries  $Q$  and entry vectors  $EV$ , our approach dynamically routes queries to appropriate clusters based on their proximity to cluster centroids. When a subset of queries  $Q_i$  are assigned to cluster  $i$ , it activates entry vectors  $EV_i$  within that cluster for distance computation. Entry vectors in other clusters are considered too distant and are excluded from the distance calculation for that particular query.

**Allocation-free and tiled FES.** The final challenge is to implement FES efficiently. A straightforward implementation might extract both  $Q_i$  and  $EV_i$  before performing distance computations. However, this approach can lead to memory allocations and copies, potentially reducing performance. To overcome this limitation, we have developed an allocation-free and tiled GPU kernel, as shown in Algorithm 2. The algorithm begins by distributing the computation across multiple GPU blocks (line 3), each handling a subset of queries and entry vectors. Within each block, the algorithm statically declares two shared memory blocks to store partial query and entry vectors (line 4). Next, each block iterates through the entry vectors and queries in a tiled manner (line 7, 12). This tiling approach is crucial for performance as it maximizes memory reads and data reuse.

Since only corresponding queries to specific entry vectors are used for distance calculations, non-active queries (those processed in other blocks) are skipped (line 9-11). This selective computation reduces unnecessary memory loads and calculations. For matching queries, the algorithm computes partial distances between the query and the entry vec-

tors (line 14). Finally, these partial distances are accumulated into the final distances array (line 15), completing the computation for the current block. The result is a highly optimized distance calculation. Like GEMM, this algorithm exploits multiple levels of parallelism, it divides the computation into tiles and performs distance computations on these smaller tiles.

Note that this tiled computational pattern, cluster-centric rather than query-centric, is specifically tailored for entry point selection. We assigns each cluster to a GPU block, which would be inefficient for traditional IVF workloads due to two factors. First, the large number of IVF buckets (typically thousands) would cause significant read amplification when processed by GPU blocks (line 3). Second, the high variance in IVF bucket sizes would lead to load imbalance, as the entire kernel must wait for the largest bucket to complete processing (line 16).

**Complexity analysis.** As listed in Table 2, distance calculations of graph traversal has time complexity of  $O(mnd)$ . For FES with  $r$  clusters, the time complexity is  $O(\frac{mnd}{r})$  as  $n$  vectors are distributed to  $r$  cells, where each query only performs  $\frac{n}{r}$  computations. When using 1 block, the FES reverts to brute force; and when there is only 1 query to process, the FES has the same complexity of graph traversal. We set  $r = 32$  to match the GPU’s warp size while obtaining a higher computational density.

## 6. Evaluation

### 6.1. Experimental Setup

The experiments were conducted on cloud virtual machines equipped with Intel Xeon Platinum 8369B CPUs and an NVIDIA A10 GPU (24 GB). We allocated 32 vCPUs (equivalent to 16 OpenMP threads) for the evaluation. Single-precision float32 is used for distance calculations on both CPU and GPU, and SIMD instructions up to AVX2 are utilized, following the performance tuning guidelines from the open source community <sup>1</sup>.

**Datasets.** We use four 100-million-scale datasets listed in Table 3, DEEP (Babenko & Lempitsky, 2016), T2I (Yandex, 2021), WIKI, and LAION (Schuhmann et al., 2022), representing both moderate and high-dimensional data that exceed typical GPU memory capacities. For the WIKI dataset, we constructed it by sampling 100 million paragraphs from English Wikipedia and generating embeddings using the BGE (Xiao et al., 2023) model, which serves as the default embedding method in the LlamaIndex (Liu, 2022) framework. We also employ smaller 1 million subsets of the same datasets (e.g., DEEP-1M) for analysis, as

<sup>1</sup><https://github.com/facebookresearch/faiss/wiki/How-to-make-Faiss-run-faster>

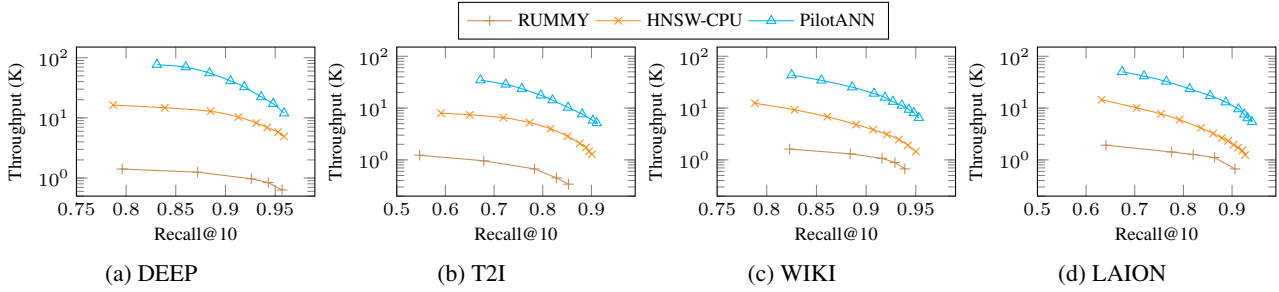


Figure 5. Recall-Throughput curves on 100 million datasets.

Table 3. Evaluation datasets.

Dataset	Index size	Smpl. / SVD ratio	GPU mem.
DEEP	59.6 GB	0.33, 1.0	19.7 GB (3.0×)
T2I	98.3 GB	0.25, 0.64	17.9 GB (5.5×)
WIKI	166.9 GB	0.25, 0.33	17.9 GB (9.3×)
LAION	288.2 GB	0.25, 0.21	19.4 GB (14.9×)

their original sizes can pose challenges.

**Baselines.** We compare PilotANN against the following state-of-the-art approaches:

- *HNSW* (Malkov & Yashunin, 2020) is the industry-standard solution known for its robust performance. We evaluate the CPU implementation from FAISS (Douze et al., 2024) 1.8.0<sup>2</sup>. To ensure a fair comparison, PilotANN utilizes the same trained graph index as FAISS without altering the training algorithms.
- *RUMMY* (Zhang et al., 2024) is a recent IVF-based (coarse clustering) approach tackling similar challenges. It shares our focus on addressing GPU memory constraints in ANNS.
- *CAGRA* (Ootomo et al., 2023), NVIDIA’s ANNS algorithm, was evaluated as an additional baseline but encountered GPU memory boundaries when processing our datasets.

**Metrics.** We focus on recall as our primary metric, measured as:  $\text{recall}@k = \frac{|\text{retrieved}_k \cap \text{groundtruth}_k|}{k}$ . In particular, we evaluate the effectiveness of PilotANN through recall-throughput curves, showing how accuracy trades off with computational performance.

## 6.2. Overall Performance

PilotANN demonstrates significant performance improvements over the baselines across all scenarios.

**Overall.** Figure 5 illustrates the throughput improvements

<sup>2</sup>Recent updates to FAISS 1.8.0 have significantly enhanced its performance, making it a strong baseline for comparison: <https://github.com/facebookresearch/faiss/pull/2841>.

Table 4. Throughput and cost-effectiveness.

Dataset	Recall@10	FAISS	PilotANN	Speedup. per \$
DEEP	0.85	14,310	81,350	3.4×
	0.90	11,514	44,586	2.3×
	0.95	6,098	16,248	1.6×
T2I	0.80	4,333	17,075	2.4×
	0.85	2,869	10,519	2.2×
	0.90	1,318	6,642	3.0×
WIKI	0.85	7,633	35,821	2.8×
	0.90	4,229	17,796	2.5×
	0.95	1,448	7,456	3.1×
LAION	0.80	5,619	25,912	2.8×
	0.85	3,632	18,063	3.0×
	0.90	2,103	11,285	3.2×

by PilotANN compared to the *HNSW-CPU* on different large scale datasets. For the 96-dimensional DEEP dataset, our method achieves a 3.9× speedup compared to the baseline. Performance gains are even more significant for other datasets, showing 5.1 – 5.4× speedups, with the benefits becoming more pronounced as vector dimensions increase. *RUMMY* is slower than *HNSW-CPU* in all scenarios because the IVF approach (which *RUMMY* utilizes) inherently necessitates more distance calculations than HNSW. Similar benefits for top-100 searches have also been observed (omit due to page limits). Notably, T2I is a known difficult evaluation (Simhadri et al., 2022), our method delivers substantial speedups, despite not being specifically optimized for this dataset.

**Cost-effectiveness.** Despite the significantly higher cost of the GPU-based platform (2.81 USD/hour) compared to the CPU-only solution (1.69 USD/hour), we achieve notable cost-effectiveness: 2.3× for DEEP, 3.0 – 3.2× for T2I, WIKI, and LAION in throughput per dollar, as illustrated in Table 4. This suggests that PilotANN excels with higher-dimensional ANNS. Given the difficulties in improving CPU capabilities, PilotANN offers a practical solution for enhancing ANNS processing capacity.

**CAGRA-UVI.** Figure 6 illustrates the comparison over

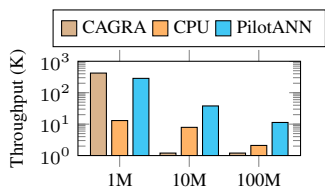


Figure 6. CAGRA on LAION dataset with UVM enabled.

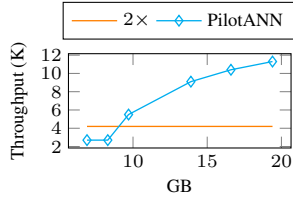


Figure 7. Minimum required GPU memory on LAION.

Table 5. Ablation study on LAION dataset.

Scheme	Throughput
PilotANN	11,285
- CPU-GPU pipelining	9,436 (-87.9%)
- Fast entry selection	8,756 (-32.3%)
- ② Residual refinement	8,479 (-13.2%)
- ① GPU piloting	2671 (-276%)
FAISS	2,103

**CAGRA.** CAGRA does not scale beyond GPU memory limits (i.e., our datasets), we switch its memory allocations to *cudaMallocManaged* (NVIDIA, 2020). This enables unified virtual memory (UVM), resulting in memory copying between the CPU and GPU when out-of-bounds access happens. For datasets that fit within GPU memory, CAGRA attains up to  $32\times$  speedup over the baseline, while PilotANN performs slightly worse because our kernel is designed to process subgraphs, resulting in additional overhead. When the dataset exceeds GPU memory, UVM usage leads to inefficient CPU-GPU data transfers, causing slowdowns on CAGRA that falls behind CPU-only approach. In contrast, PilotANN demonstrates scalability in handling growing datasets.

**Minimum GPU memory requirement.** We evaluate the scalability of PilotANN by determining the minimum GPU memory needed to achieve speedup. We allocate up to 81% of the available GPU memory (Table 3) for the graph index and vectors, reserving the remaining for dynamic allocations during query processing (e.g., query vectors and candidate sets). Experiments with the LAION dataset demonstrates PilotANN’s exceptional scalability. With 19.4 GB GPU memory, we achieve a  $4.8\times$  throughput speedup while processing a dataset  $14.9\times$  larger than the the memory allocated. As we decrease the GPU memory to 9.7 GB (dataset  $29.7\times$  larger), the system still maintains a  $2.6\times$  speedup. As our approach is complementary to quantization techniques, future integration could enable even greater scalability.

### 6.3. Component Analysis

**Ablation study.** We conducted an ablation study on the LAION dataset to evaluate CPU-GPU pipelining, fast entry

selection, and the multi-stage processing. As shown in Table 5, we sequentially removed each component and found that all components contribute positively to system performance. Among these, the GPU piloting stage demonstrates the most substantial impact with a 276% improvement. Even when all components were removed, leaving only a naive CPU-only greedy search implementation, PilotANN maintains a  $1.27\times$  speedup due to our hand-optimized AVX2 implementation.

Additional analyses can be found in Appendix §A.

## 7. Related Work

### 7.1. Large-scale ANNS

Prior ANNS research focused primarily on index structure and data encoding optimizations, the Inverted Multi-Index (IMI) (Babenko & Lempitsky, 2015) enhanced space partitioning through multi-codebook quantization, while PQFastScan (André et al., 2016) improved performance via SIMD and cache-aware optimizations. FAISS (Douze et al., 2024), a widely-adopted ANNS library, scales effectively to RAM capacity but has limited GPU support. DiskANN (Jayaram Subramanya et al., 2019) and SPANN (Chen et al., 2021) introduced novel disk-based indexing for billion-scale datasets, addressing different but related memory hierarchy challenges compared to our work. PilotANN is orthogonal to quantization and disk-based approaches, suggesting potential future integration of both approaches.

### 7.2. GPU-accelerated ANNS

Several approaches have leveraged GPUs for ANNS acceleration. RUMMY (Zhang et al., 2024) implemented CPU-GPU pipelining for IVF-based search, though this strategy is suboptimal for graph-based indexes. SONG (Zhao et al., 2020) and CAGRA (Ootomo et al., 2023) achieved significant speedups through GPU parallelization but their methods are constrained by GPU memory capacity. BANG (Karthik et al., 2024) handled billion-scale datasets using hybrid CPU-GPU processing but lacking CPU baseline comparisons<sup>3</sup>. In contrast, PilotANN presents a memory-bounded GPU acceleration framework that effectively utilizes commodity GPUs while overcoming their memory constraints. In addition, PilotANN also maintains full compatibility with existing CPU systems and achieves significant speedups without compromising search accuracy or requiring high-end GPU hardware.

<sup>3</sup>Our claims may be outdated, as BANG is a work in progress.



## 8. Conclusion

This work introduces a novel graph-based ANNS system that effectively utilizes both CPU and GPU for emerging ANNS workloads. By decomposing top- $k$  search into a multi-stage CPU-GPU pipeline and employing efficient entry selection, our system achieves significant performance improvements over existing CPU-only approaches.

## Impact Statement

The effectiveness and efficiency of our proposed PilotANN system democratizes high-performance nearest neighbor search by achieving competitive performance with just a single commodity GPU. Our design significantly reduces computational overhead, making advanced search capabilities accessible to researchers and organizations with limited computing resources. Unlike existing solutions that require expensive high-end GPUs, our approach enables efficient ANNS deployment on common hardware setups while maintaining search accuracy. This work contributes to sustainable AI infrastructure development and empowers broader adoption of ANNS technology across diverse applications, especially for recent generative AIs.

## References

- André, F., Kermarrec, A.-M., and Le Scouarnec, N. Cache locality is not enough: High-performance nearest neighbor search with product quantization fast scan. In *42nd International Conference on Very Large Data Bases*, volume 9, pp. 12, 2016.
- Babenko, A. and Lempitsky, V. S. The inverted multi-index. *IEEE Trans. Pattern Anal. Mach. Intell.*, 37(6):1247–1260, 2015. doi: 10.1109/TPAMI.2014.2361319. URL <https://doi.org/10.1109/TPAMI.2014.2361319>.
- Babenko, A. and Lempitsky, V. S. Efficient indexing of billion-scale datasets of deep descriptors. In *2016 IEEE Conference on Computer Vision and Pattern Recognition, CVPR 2016, Las Vegas, NV, USA, June 27-30, 2016*, pp. 2055–2063. IEEE Computer Society, 2016. doi: 10.1109/CVPR.2016.226. URL <https://doi.org/10.1109/CVPR.2016.226>.
- Bang, F. Gptcache: An open-source semantic cache for llm applications enabling faster answers and cost savings. In *Proceedings of the 3rd Workshop for Natural Language Processing Open Source Software (NLP-OSS 2023)*, pp. 212–218, 2023.
- Blattmann, A., Rombach, R., Oktay, K., Müller, J., and Ommer, B. Retrieval-augmented diffusion models. *Advances in Neural Information Processing Systems*, 35: 15309–15324, 2022.
- Chen, Q., Zhao, B., Wang, H., Li, M., Liu, C., Li, Z., Yang, M., and Wang, J. SPANN: highly-efficient billion-scale approximate nearest neighborhood search. In Ranzato, M., Beygelzimer, A., Dauphin, Y. N., Liang, P., and Vaughan, J. W. (eds.), *Advances in Neural Information Processing Systems 34: Annual Conference on Neural Information Processing Systems 2021, NeurIPS 2021, December 6-14, 2021, virtual*, pp. 5199–5212, 2021. URL <https://proceedings.neurips.cc/paper/2021/hash/299dc35e747eb77177d9cea10a802da2-Abstract.html>.
- Covington, P., Adams, J., and Sargin, E. Deep neural networks for youtube recommendations. In *Proceedings of the 10th ACM conference on recommender systems*, pp. 191–198, 2016.
- Devlin, J., Chang, M.-W., Lee, K., and Toutanova, K. Bert: Pre-training of deep bidirectional transformers for language understanding. *arXiv preprint arXiv:1810.04805*, 2018.
- Dong, W., Charikar, M., and Li, K. Efficient k-nearest neighbor graph construction for generic similarity measures. In Srinivasan, S., Ramamritham, K., Kumar, A., Ravindra, M. P., Bertino, E., and Kumar, R. (eds.), *Proceedings of the 20th International Conference on World Wide Web, WWW 2011, Hyderabad, India, March 28 - April 1, 2011*, pp. 577–586. ACM, 2011. doi: 10.1145/1963405.1963487. URL <https://doi.org/10.1145/1963405.1963487>.
- Dosovitskiy, A., Beyer, L., Kolesnikov, A., Weissenborn, D., Zhai, X., Unterthiner, T., Dehghani, M., Minderer, M., Heigold, G., Gelly, S., Uszkoreit, J., and Houshy, N. An image is worth 16x16 words: Transformers for image recognition at scale. In *9th International Conference on Learning Representations, ICLR 2021, Virtual Event, Austria, May 3-7, 2021*. OpenReview.net, 2021. URL <https://openreview.net/forum?id=YicbFdNTTy>.
- Douze, M., Sablayrolles, A., and Jégou, H. Link and code: Fast indexing with graphs and compact regression codes. In *2018 IEEE Conference on Computer Vision and Pattern Recognition, CVPR 2018, Salt Lake City, UT, USA, June 18-22, 2018*, pp. 3646–3654. Computer Vision Foundation / IEEE Computer Society, 2018. doi: 10.1109/CVPR.2018.00384. URL [http://openaccess.thecvf.com/content\\_cvpr\\_2018/html/Douze\\_Link\\_and\\_Code\\_CVPR\\_2018\\_paper.html](http://openaccess.thecvf.com/content_cvpr_2018/html/Douze_Link_and_Code_CVPR_2018_paper.html).

- Douze, M., Guzhva, A., Deng, C., Johnson, J., Szilvasy, G., Mazaré, P., Lomeli, M., Hosseini, L., and Jégou, H. The faiss library. *CoRR*, abs/2401.08281, 2024. doi: 10.48550/ARXIV.2401.08281. URL <https://doi.org/10.48550/arXiv.2401.08281>.
- Fu, C., Xiang, C., Wang, C., and Cai, D. Fast approximate nearest neighbor search with the navigating spreading-out graph. *Proc. VLDB Endow.*, 12(5):461–474, 2019. doi: 10.14778/3303753.3303754. URL <http://www.vldb.org/pvldb/vol12/p461-fu.pdf>.
- Gionis, A., Indyk, P., and Motwani, R. Similarity search in high dimensions via hashing. In Atkinson, M. P., Orłowska, M. E., Valduriez, P., Zdonik, S. B., and Brodie, M. L. (eds.), *VLDB’99, Proceedings of 25th International Conference on Very Large Data Bases, September 7-10, 1999, Edinburgh, Scotland, UK*, pp. 518–529. Morgan Kaufmann, 1999. URL <http://www.vldb.org/conf/1999/P49.pdf>.
- Gordo, A., Almazán, J., Revaud, J., and Larlus, D. Deep image retrieval: Learning global representations for image search. In *Computer Vision—ECCV 2016: 14th European Conference, Amsterdam, The Netherlands, October 11-14, 2016, Proceedings, Part VI 14*, pp. 241–257. Springer, 2016.
- Hajebi, K., Abbasi-Yadkori, Y., Shahbazi, H., and Zhang, H. Fast approximate nearest-neighbor search with k-nearest neighbor graph. In Walsh, T. (ed.), *IJCAI 2011, Proceedings of the 22nd International Joint Conference on Artificial Intelligence, Barcelona, Catalonia, Spain, July 16-22, 2011*, pp. 1312–1317. IJCAI/AAAI, 2011. doi: 10.5591/978-1-57735-516-8/IJCAI11-222. URL <https://doi.org/10.5591/978-1-57735-516-8/IJCAI11-222>.
- He, X., Liao, L., Zhang, H., Nie, L., Hu, X., and Chua, T.-S. Neural collaborative filtering. In *Proceedings of the 26th international conference on world wide web*, pp. 173–182, 2017.
- Jayaram Subramanya, S., Devvrit, F., Simhadri, H. V., Krishnawamy, R., and Kadekodi, R. Diskann: Fast accurate billion-point nearest neighbor search on a single node. *Advances in Neural Information Processing Systems*, 32, 2019.
- Jégou, H., Douze, M., and Schmid, C. Product quantization for nearest neighbor search. *IEEE Trans. Pattern Anal. Mach. Intell.*, 33(1):117–128, 2011a. doi: 10.1109/TPAMI.2010.57. URL <https://doi.org/10.1109/TPAMI.2010.57>.
- Jégou, H., Tavenard, R., Douze, M., and Amsaleg, L. Searching in one billion vectors: Re-rank with source coding. In *Proceedings of the IEEE International Conference on Acoustics, Speech, and Signal Processing, ICASSP 2011, May 22-27, 2011, Prague Congress Center, Prague, Czech Republic*, pp. 861–864. IEEE, 2011b. doi: 10.1109/ICASSP.2011.5946540. URL <https://doi.org/10.1109/ICASSP.2011.5946540>.
- Karthik, V., Khan, S., Singh, S., Simhadri, H. V., and Vedula, J. Bang: Billion-scale approximate nearest neighbor search using a single gpu. *arXiv e-prints*, pp. arXiv–2401, 2024.
- Kulis, B. and Grauman, K. Kernelized locality-sensitive hashing for scalable image search. In *2009 IEEE 12th international conference on computer vision*, pp. 2130–2137. IEEE, 2009.
- Lewis, P. S. H., Perez, E., Piktus, A., Petroni, F., Karpukhin, V., Goyal, N., Küttler, H., Lewis, M., Yih, W., Rocktäschel, T., Riedel, S., and Kiela, D. Retrieval-augmented generation for knowledge-intensive NLP tasks. In Larochelle, H., Ranzato, M., Hadsell, R., Balcan, M., and Lin, H. (eds.), *Advances in Neural Information Processing Systems 33: Annual Conference on Neural Information Processing Systems 2020, NeurIPS 2020, December 6-12, 2020, virtual*, 2020. URL <https://proceedings.neurips.cc/paper/2020/hash/6b493230205f780e1bc26945df7481e5-Abstract.html>.
- Liu, J. LlamaIndex, 11 2022. URL [https://github.com/jerryjliu/llama\\_index](https://github.com/jerryjliu/llama_index).
- Lu, K., Kudo, M., Xiao, C., and Ishikawa, Y. Hvs: hierarchical graph structure based on voronoi diagrams for solving approximate nearest neighbor search. *Proc. VLDB Endow.*, 15(2):246–258, October 2021. ISSN 2150-8097. doi: 10.14778/3489496.3489506. URL <https://doi.org/10.14778/3489496.3489506>.
- Malkov, Y., Ponomarenko, A., Logvinov, A., and Krylov, V. Approximate nearest neighbor algorithm based on navigable small world graphs. *Information Systems*, 45: 61–68, 2014.
- Malkov, Y. A. and Yashunin, D. A. Efficient and robust approximate nearest neighbor search using hierarchical navigable small world graphs. *IEEE Trans. Pattern Anal. Mach. Intell.*, 42(4):824–836, 2020. doi: 10.1109/TPAMI.2018.2889473. URL <https://doi.org/10.1109/TPAMI.2018.2889473>.
- NVIDIA. Fast, Flexible Allocation for NVIDIA CUDA with RAPIDS Memory Manager — NVIDIA Technical Blog — [developer.nvidia.com](https://developer.nvidia.com).

- <https://developer.nvidia.com/blog/fast-flexible-allocation-for-cuda-with-rapchorage-alaska-usa>. 2020. [Accessed 15-10-2024].
- Ootomo, H., Naruse, A., Nolet, C., Wang, R., Feher, T., and Wang, Y. CAGRA: highly parallel graph construction and approximate nearest neighbor search for gpus. *CoRR*, abs/2308.15136, 2023. doi: 10.48550/ARXIV.2308.15136. URL <https://doi.org/10.48550/arXiv.2308.15136>.
- Peng, Z., Zhang, M., Li, K., Jin, R., and Ren, B. iqan: Fast and accurate vector search with efficient intra-query parallelism on multi-core architectures. In Dehnavi, M. M., Kulkarni, M., and Krishnamoorthy, S. (eds.), *Proceedings of the 28th ACM SIGPLAN Annual Symposium on Principles and Practice of Parallel Programming, PPOPP 2023, Montreal, QC, Canada, 25 February 2023 - 1 March 2023*, pp. 313–328. ACM, 2023. doi: 10.1145/3572848.3577527. URL <https://doi.org/10.1145/3572848.3577527>.
- Radford, A., Kim, J. W., Hallacy, C., Ramesh, A., Goh, G., Agarwal, S., Sastry, G., Askell, A., Mishkin, P., Clark, J., Krueger, G., and Sutskever, I. Learning transferable visual models from natural language supervision. In Meila, M. and Zhang, T. (eds.), *Proceedings of the 38th International Conference on Machine Learning, ICML 2021, 18-24 July 2021, Virtual Event*, volume 139 of *Proceedings of Machine Learning Research*, pp. 8748–8763. PMLR, 2021. URL <http://proceedings.mlr.press/v139/radford21a.html>.
- Schuhmann, C., Beaumont, R., Vencu, R., Gordon, C., Wightman, R., Cherti, M., Coombes, T., Katta, A., Mullis, C., Wortsman, M., Schramowski, P., Kundurthy, S., Crowson, K., Schmidt, L., Kaczmarczyk, R., and Jitsev, J. LAION-5B: an open large-scale dataset for training next generation image-text models. In Koyejo, S., Mohamed, S., Agarwal, A., Belgrave, D., Cho, K., and Oh, A. (eds.), *Advances in Neural Information Processing Systems 35: Annual Conference on Neural Information Processing Systems 2022, NeurIPS 2022, New Orleans, LA, USA, November 28 - December 9, 2022*, 2022. URL [http://papers.nips.cc/paper\\_files/paper/2022/hash/a1859debf3b59d094f3504d5ebb6c25-Abstract-and\\_Benchmarks.html](http://papers.nips.cc/paper_files/paper/2022/hash/a1859debf3b59d094f3504d5ebb6c25-Abstract-and_Benchmarks.html).
- Schütze, H., Manning, C. D., and Raghavan, P. *Introduction to information retrieval*, volume 39. Cambridge University Press Cambridge, 2008.
- Silpa-Anan, C. and Hartley, R. I. Optimised kd-trees for fast image descriptor matching. In *2008 IEEE Computer Society Conference on Computer Vision and Pattern Recognition (CVPR 2008)*, 24-26 June 2008, Anchorage, Alaska, USA. IEEE Computer Society, 2008. doi: 10.1109/CVPR.2008.4587638. URL <https://doi.org/10.1109/CVPR.2008.4587638>.
- Simhadri, H. V., Williams, G., Aumüller, M., Douze, M., Babenko, A., Baranchuk, D., Chen, Q., Hosseini, L., Krishnaswamny, R., Srinivasa, G., Subramanya, S. J., and Wang, J. Results of the neurips’21 challenge on billion-scale approximate nearest neighbor search. In Kiela, D., Ciccone, M., and Caputo, B. (eds.), *Proceedings of the NeurIPS 2021 Competitions and Demonstrations Track*, volume 176 of *Proceedings of Machine Learning Research*, pp. 177–189. PMLR, 06–14 Dec 2022. URL <https://proceedings.mlr.press/v176/simhadri22a.html>.
- Williams, S., Waterman, A., and Patterson, D. A. Roofline: an insightful visual performance model for multicore architectures. *Commun. ACM*, 52(4):65–76, 2009. doi: 10.1145/1498765.1498785. URL <https://doi.org/10.1145/1498765.1498785>.
- Xiao, S., Liu, Z., Zhang, P., and Muennighoff, N. C-pack: Packaged resources to advance general chinese embedding, 2023.
- Yandex. Yandex — [research.yandex.com](https://research.yandex.com). <https://research.yandex.com/blog/benchmarks-for-billion-scale-similarity-search>, 2021. [Accessed 15-10-2024].
- Yang, J., Yi, X., Zhiyuan Cheng, D., Hong, L., Li, Y., Xiaoming Wang, S., Xu, T., and Chi, E. H. Mixed negative sampling for learning two-tower neural networks in recommendations. In *Companion proceedings of the web conference 2020*, pp. 441–447, 2020.
- Zhang, Z., Liu, F., Huang, G., Liu, X., and Jin, X. Fast vector query processing for large datasets beyond {GPU} memory with reordered pipelining. In *21st USENIX Symposium on Networked Systems Design and Implementation (NSDI 24)*, pp. 23–40, 2024.
- Zhao, W., Tan, S., and Li, P. SONG: approximate nearest neighbor search on GPU. In *36th IEEE International Conference on Data Engineering, ICDE 2020, Dallas, TX, USA, April 20-24, 2020*, pp. 1033–1044. IEEE, 2020. doi: 10.1109/ICDE48307.2020.00094. URL <https://doi.org/10.1109/ICDE48307.2020.00094>.
- Zhou, W., Lu, Y., Li, H., and Tian, Q. Scalar quantization for large scale image search. In *Proceedings of the 20th ACM international conference on Multimedia*, pp. 169–178, 2012.

Zhu, Y. RTNN: accelerating neighbor search using hardware ray tracing. In Lee, J., Agrawal, K., and Spear, M. F. (eds.), *PPoPP '22: 27th ACM SIGPLAN Symposium on Principles and Practice of Parallel Programming, Seoul, Republic of Korea, April 2 - 6, 2022*, pp. 76–89. ACM, 2022. doi: 10.1145/3503221.3508409. URL <https://doi.org/10.1145/3503221.3508409>.

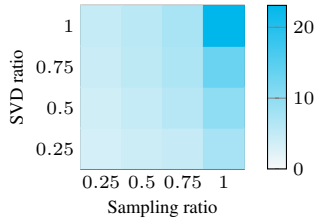


Figure 8. Speedup on different GPU piloting configuration.

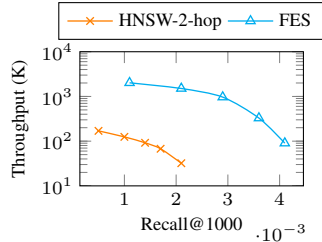


Figure 9. FES benefit.

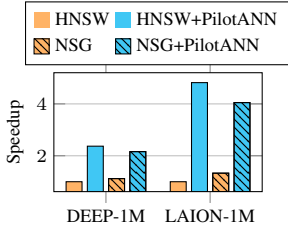


Figure 10. HNSW v.s. NSG.

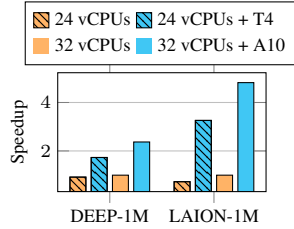


Figure 11. T4 v.s. A10.

## A. Appendix

### A.1. Component Analysis

We evaluate the effectiveness of our proposed techniques.

**GPU piloting analysis.** To handle large graph index within limited GPU memory, PilotANN employs subgraph sampling and dimensionality reduction (§4). We evaluate how graph sampling and dimension reduction impact system performance on the LAION-1M dataset. When using the full graph and original vectors (sampling and SVD ratio = 1.0) in GPU-only search, we observe a maximum speedup of  $23.1\times$  compared to the CPU baseline. Using dimension reduction only (ratio = 0.25) achieves a  $7.5\times$  speedup, while using sampling only (ratio = 0.25) yields a  $4.9\times$  speedup. This asymmetric impact suggests that our method tolerates aggressive dimension reduction while requiring a higher sampling ratio to maintain search quality.

**FES analysis.** We evaluate the effectiveness of FES (§5) on the LAION-1M dataset using top-1000 recall as our metric, with the first 2-hop traversal of HNSW as the baseline, both evaluated on the GPU. FES achieves 2017.0K QPS to reach a top-1000 recall of 0.001. This throughput represents a  $16.2\times$  speedup compared to the graph traversal baseline, which only obtains 124.7K QPS. These results demonstrate that FES significantly improves both entry point quality and computational efficiency, making it a crucial component of PilotANN.

### A.2. Sensitivity Analysis

To explore the sensitivity, we conducted more studies on the 1M datasets. The analysis highlights key observations regarding consistent benefits across graph construction methods and hardware settings.

**Graph construction.** PilotANN demonstrates orthogonality to graph construction methods, we compare the speedup using both HNSW and NSG graph construction methods. While both combinations showed significant improvements over their baseline counterparts, PilotANN+HNSW achieved higher speedups of  $2.4\times$  and  $4.8\times$  on DEEP-1M and LAION-1M respectively, compared to  $2.2\times$  and  $4.1\times$  of PilotANN+NSG. This is because NSG brings better search efficiency to the baseline, as the search quality and performance improve, different methods converge, leaving less room for relative improvements.

**Hardware independence.** To validate the broad applicability of PilotANN, we evaluated the system on Intel Xeon Platinum 8163 CPUs paired with an older NVIDIA T4 GPU, achieving  $1.9\times$  and  $4.5\times$  speedups on DEEP-1M and LAION-1M respectively, compared to  $2.4\times$  and  $4.8\times$  on our primary A10 test platform. While the speedups are moderately lower on the T4 due to its reduced GPU compute capacity and PCIe bandwidth, the consistent benefits across both platforms confirm PilotANN’s adaptability to different hardware architectures.

### A.3. Implementation

PilotANN is primarily built from scratch, comprising about 3.5K lines of Python, 1K lines of C++, and 1K lines of CUDA code. This implementation was necessary due to the challenges in reusing existing ANNS libraries for CPU-GPU collaborating. Notably, the system is implemented as an extension of LibTorch, which allows us to leverage the powerful tensor library for efficient CPU-GPU data management, facilitating seamless integration with deep learning models. The CPU kernel matches the performance of the latest FAISS implementation, while the GPU kernel has been tailored to handle subgraph traversal, demonstrating improved capabilities over existing implementations.